AN INTEGRATED APPROACH TO FLOW, THERMAL AND MECHANICAL MODELING OF ELECTRONICS DEVICES

John Parry, Chris Marooney
Flomerics Limited
Bridge Road, Hampton Court
Surrey, UK
Email: john.parry@flomerics.co.uk

Matt Warner, Chris Bailey, Koulis Pericleous
Centre for Numerical Modelling and Process Analysis
University of Greenwich
Greenwich, London, UK.
Email: c.bailey@gre.ac.uk

ABSTRACT

The future success of many electronics companies will depend to a large extent on their ability to initiate techniques that bring schedules, performance, tests, support, production, life-cycle-costs, reliability prediction and quality control into the earliest stages of the product creation process. Earlier papers [1, 2] have discussed the benefits of an integrated analysis environment for system-level thermal, stress and EMC prediction. This paper focuses on developments made to the stress analysis module and presents results obtained for an SMT resistor. Lifetime predictions are made using the Coffin-Manson equation. Comparison with the creep strain energy based models of Darveaux [3] shows the shear strain based method to underestimate the solder joint life. Conclusions are also made about the capabilities of both approaches to predict the qualitative and quantitative impact of design changes.

Keywords: Multiphysics, Modeling, CFD, FE, Thermal, Stress, Reliability, Thermomechanical.

INTRODUCTION - TOWARDS A MULTIPHYSICS MODELING APPROACH.

Increasing global competition is a significant factor impacting the design of modern electronic products. The product development time for electronic systems in the early 1980s was often years. Today time-to-market is only a few months. Experimentally validated computational modeling has become the preferred choice for rapidly carrying out numerous 'what-if' studies during design and the need for such an integrated modeling approach is emphasised in the Semiconductor Industry Association's 1997 Roadmap document [4].

Flomerics is developing novel technologies that will provide a unified modelling framework for thermal, mechanical, and electromagnetic predictions. This multi-physics methodology is based on numerical algorithms that use current best-in-class techniques that are integrated in an efficient and robust manner. Figure 1 illustrates the relationship between the existing CFD tool and those under development – a stress module and an EMC tool, which will respectively provide predictions of the thermally induced stresses and electromagnetic fields within and emitted by electronic systems.

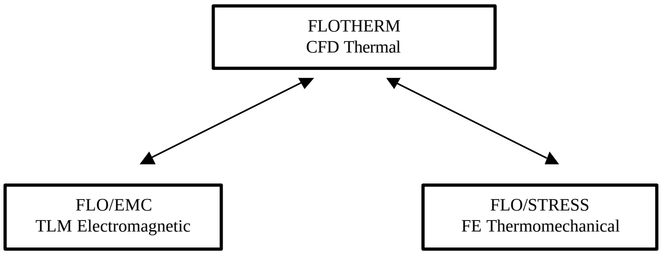

Fig. 1: Multidisciplinary Modeling Environment

The tight integration between the tools will provide users with a common user interface that facilitates the ease of model building and the interpretation of the results. Eventually the system will use a common data model for storage of all geometrical and simulation data allowing a single model to be analysed in many ways.

The system will require sophisticated algorithms to enable it to correctly interpret the input for the various solver modules. For example, in the CFD analysis the main characteristic of a fan is its air moving ability. In EMC analysis air movement is irrelevant. However, the fan represents an annular aperture in the casing through which electromagnetic radiation is exchanged with the surroundings (particularly when it has plastic blades). Understanding the mapping of objects between the analysis types is one of the big challenges for the development of a common data model. This paper focuses on recent developments for the stress analysis module.

INTEGRATION OF THE STRESS MODULE

The integration of the stress module with the CFD enables a stress analysis of an electronic assembly to be performed within the thermal design software environment. The stress analysis module uses the CFD model, mesh and temperature results of the selected assembly. The two illustrative examples discussed below both consider a package-board assembly being subjected to a temperature cycle. However, to predict the reliability of the assembly under functional cycling or operational conditions, it is critically important to use the temperature field predicted by the CFD, since the part is generally hotter than the board, and the temperature of, and temperature distribution within the part and board affect both their relative expansion and warpage.

Within the selected assembly, only the mesh in the solid regions is of interest for the stress calculation. Figure 2 summarizes the input data and results generated by the CFD and FE analyses.

CFD Thermal Tool		**Stress Solver**
Data and Solution: • Fluid and Solid Regions • Structured Mesh in Solid and Fluid Regions • Finite Volume Solver Results: • Fluid Velocities • Temperatures Derived Quantities: • Fan Operating Point	➔	Data and Solution: • Solid Regions Only • Unstructured Mesh in Solid Regions • Finite Element Solver Results: • Solid Displacements • Stresses and Strains Derived Quantities: • Principal Stresses

Fig. 2: Integration between CFD and Stress

Geometry, grid and temperature information is passed from the CFD solver to the FE solver at the end of the CFD calculation. Results from the stress analysis are available for the post-processing environment used by the CFD tool, allowing graphical visualization of the results, profile plots and access to the elemental values.

The stress equations solved in the stress solver are discretized using traditional finite element procedures, where the change in temperature predicted by the thermal analysis is used to calculate the solid deformation. Care has been taken to ensure that very little extra work is required to provide the capability to undertake a fast stress calculation based on the predicted thermal gradients. No extra model build or meshing is required. Although the mesh used within the stress calculation is unstructured it is built up from the structured CFD mesh used for that particular assembly. The only additional input is the relevant materials data and boundary conditions required for the stress calculation. Material properties can be input as isotropic or orthotropic, and can be temperature-dependent.

ILLUSTRATIVE EXAMPLES

Previous Illustrative Example

The previous illustrative example was the Motorola PowerPC™ 604 C4/CBGA mounted on a 2-inch test coupon in a computational wind tunnel [5]. In the model, the joint was modeled as cuboidal, having the same cross-sectional area and height as the cylindrical solder joint, encapsulating the high melting point Sn10/Pb90 solder ball. The volume of the Sn10/Pb90 and Sn63/Pb37 solder are also preserved, with the Sn63/Pb37 solder being distributed equally above and below the Sn10/Pb90 solder. A schematic giving a cross-section through the model of this package is shown in the Figure 3. In this previously reported work, the stress solver used 8-node brick elements to replicate the mesh in the solid.

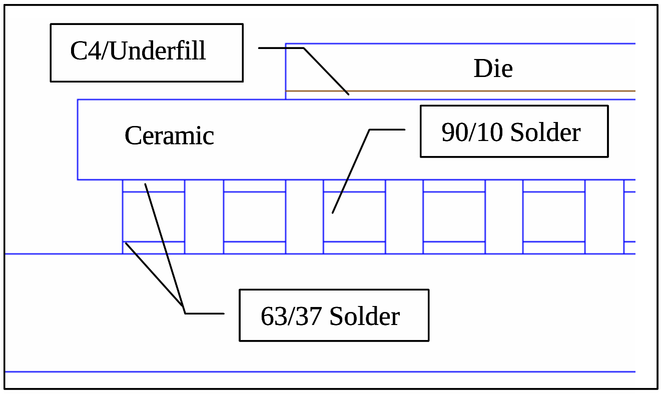

Fig. 3: CBGA Showing Detail of Solder Ball Model

The motivation for this earlier study was to investigate whether a shear strain based approach to lifetime prediction could provide results that were sufficiently accurate to use in product design. This was also the motivation for the current work.

Current Illustrative Example

The use of 8-node brick elements to replicate the CFD cells is not a limitation of the stress solver, which uses standard unstructured mesh technology. In the example reported here, both 8-node brick and 6-node wedge elements have been used to accurately represent the shape of the solder fillet.

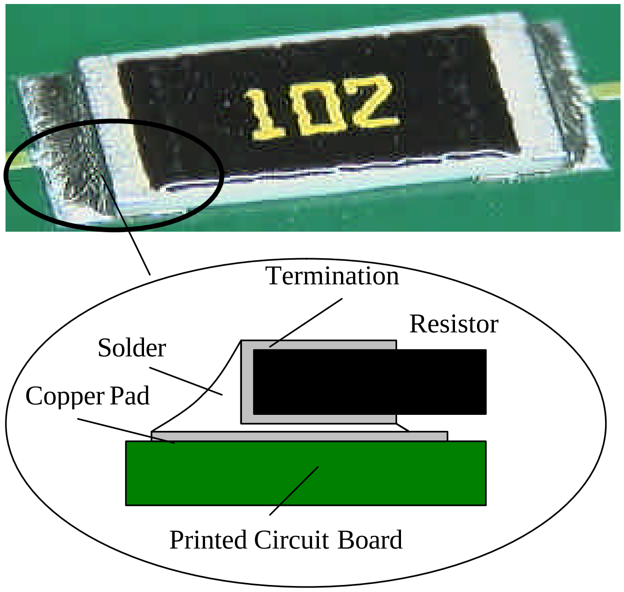

Fig. 4: Surface Mount Leadless Ceramic Resistor (LCR)

The example being considered is a surface mount leadless ceramic resistor (LCR) that has been the subject of a large-scale experimental program currently underway at the National Physical Laboratory to investigate the effect of different thermal cycles on both tin-lead and lead-free solder joints for LCR, shown in Figure 4, after Lu et al.[6].

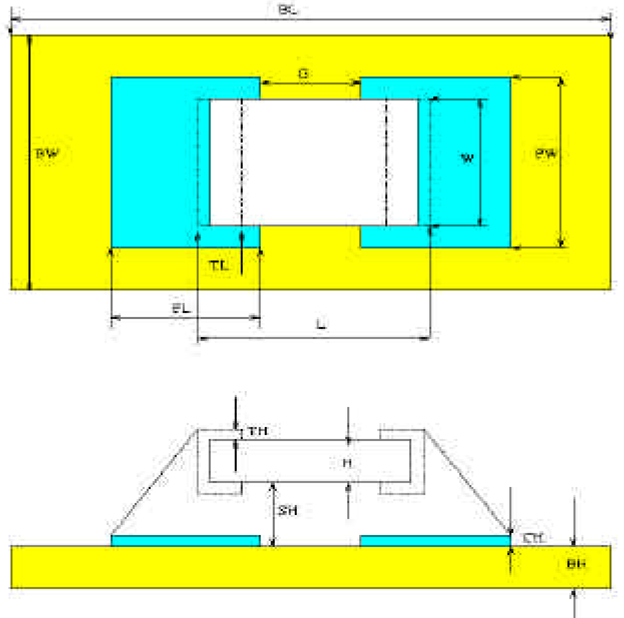

L	6.21mm
W	3.11mm (width)
TL	0.56mm (termination)
H	0.55mm (thickness)
SH	80 micons, (standoff height)
G	4.45 mm (gap)
PL	1.68 mm (pad length)
PW	3.15 mm (pad width)
BL	16 mm
BW	8 mm
TH	20+5 microns
CH	35 microns
BH	1.6 mm

Fig. 5: Schematic Drawing and Dimensions of LCR

Table 1: Mechanical properties used for the LCR.

Material	**E (GPa)**	**Poisson's ratio**	**CTE (ppm)**
60Sn-40Pb (solder)	10	0.4	21
Alumina (resistor)	282.7	0.222	6
Cu (pad)	121	0.35	17
Epoxy (underfill)	6	0.35	30
FR4 (PCB)	22	0.28	18(xy), 70(z)
Ag (termination)	83	0.37	18.9

With only two connections to the PCB, resistors are much simpler components to model, compared to multi-interconnection components such as ball grid array and flip-chip packages. Nonetheless, the reliability these two connections is no less a challenge to model in terms of accurately predicting thermal-mechanical fatigue of the solder joints – one of the main factors influencing reliability of these components. Important parameters that will influence this failure are solder volume, fillet shape, standoff height, and component material properties (i.e. Young's Modulus, Coefficient of Thermal Expansion, etc.). The influence of all these parameters can be fully investigated using advanced numerical modeling techniques.

As the resistor and the PCB are made from materials with different coefficients of thermal expansion (CTE), cyclic temperature changes will produce cyclic stress and strains in the solder joints and these cyclic loads may lead to crack initiation and propagation. It should be noted that other failure mechanisms can occur, such as resistor cracking or delamination at material interfaces. However, this modeling analysis only considers solder fatigue. The extent of the model is shown in Figure 6.

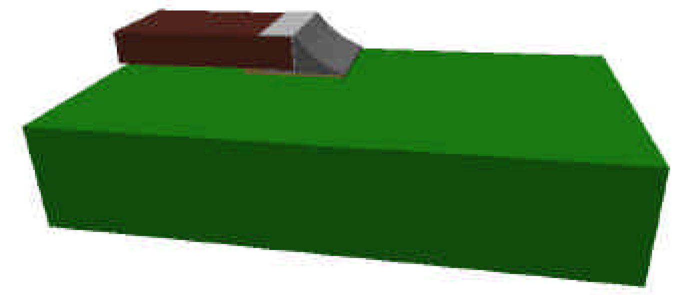

Fig. 6: Extent of Computational Model

Through the use of wedge elements, the stress solver is able to accurately capture the shape of the solder joint, modeled as shown in Figure 7.

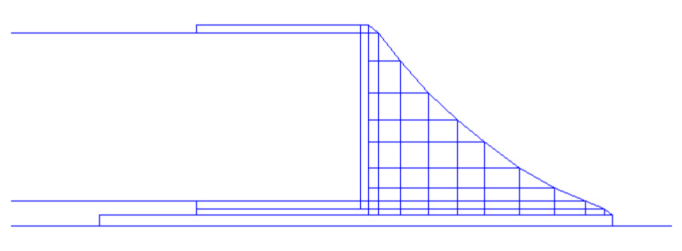

Fig. 7: Side Elevation Showing Solder Joint Detail

Note that diagram above shows the overlapping cuboids and prisms used to capture the shape of the solder joint in the CFD tool. The mesh used to model the thermomechanical behaviour of the assembly is finer than that required to represent the objects shown above.

The CFD uses a structured Cartesian mesh to represent the geometry. Structured meshes provide considerable benefits over unstructured meshes, in terms of their per-cell computational speed and memory requirements, thereby allowing much larger models to be solved. The CFD uses a porosity treatment is used to approximate the shape of the sloping surface, together with special practices to ensure the solid/fluid interaction for friction and heat transfer are accurately represented. However, the mesh itself it does not follow the surface shape, making it unsuitable for capturing the thermally induced stresses in the solid. Consequently, a novel treatment has been used to further discretize the mesh using wedge elements as shown schematically in Figure 8 below. This technique allows the solid/fluid interface to be accurately captured irrespective of how the sloping surface cuts through the CFD mesh.

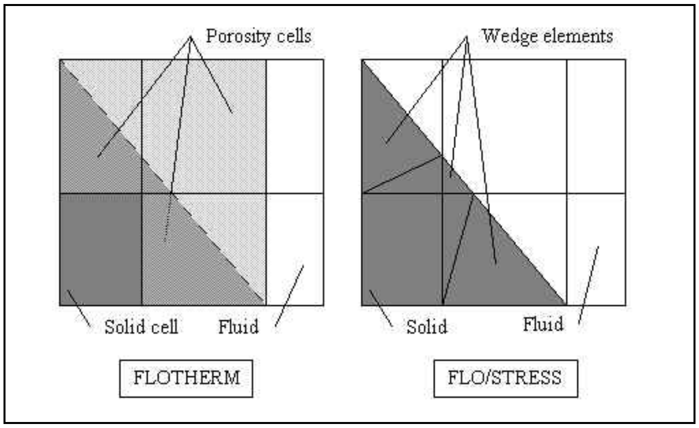

Fig. 8: Prism treatments used in CFD and stress module.

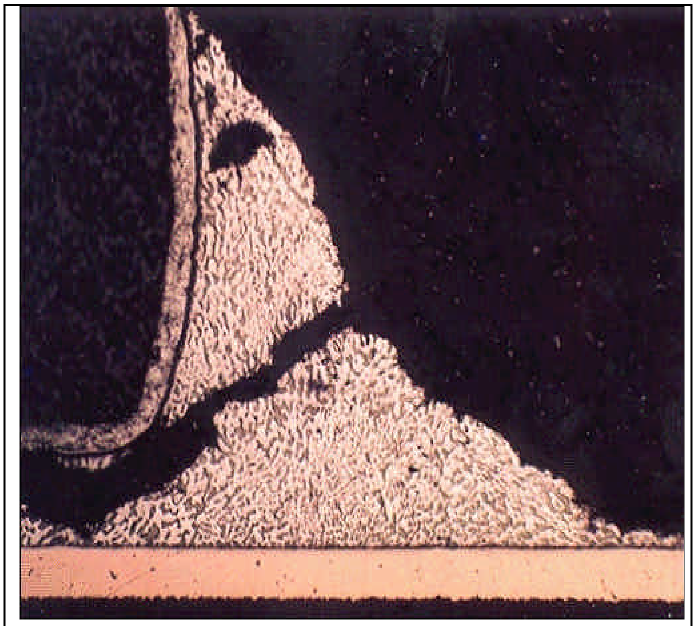

Fig. 9: Micrograph Showing Crack Through Solder Fillet

Figure 9 is a micrograph showing a cross section of the solder joint of one of these resistors that failed during a thermal cycling test. Experimental observation for tin-lead solder interconnections indicates that the cracks in the solder joints of this resistor usually initiate in the solder between the resistor body and the PCB. This crack then propagates through the solder fillet to eventually emerge on the surface of the solder fillet to cause total detachment between the resistor and the rest of the circuits on the PCB.

Previous work, Lu et al.[6], modeled the LCR using the PHYSICA modeling framework [7]. PHYSICA, developed at the University of Greenwich, is capable of simulating fluid flow including turbulence, heat transfer with solidification, and stress using the same computational mesh. Lu et al. [6] used an elasto-viscoplastic constitutive law to represent the time dependent creep behavior of the solder, treating all other materials as elastic and isotropic, with the exception of the board, which was treated as orthotropic. Lifetime models, based on the accumulated creep strain energy predicted in the solder during a thermal cycle, were then used to estimate the number of cycles to failure for a number of different cycle profiles.

This earlier work revealed that the region displaying high damage (creep strain energy) is at the edge of the device - situated between the termination and pad at the corner away from the symmetry plane. This predicted location of high damage indicates the most likely spot for crack initiation. The prediction is consistent with experimental observations, which also appear to suggest that this is the location for crack initiation. After initiation, the crack will first propagate through the whole area between the pad and resistor, and then propagate into the fillet mass - eventually causing total failure of the solder joint. In light of this observation, the total lifetime was calculated in two steps. In the first step, the average value of the creep strain energy dissipated per cycle was calculated for the solder volume between the pad on the PCB and the termination on the resistor, shown as V1 in Figure 10. In the second step a new model was constructed with the solder between the PCB and resistor removed. The creep strain energy dissipated per cycle was then calculated for the solder in the fillet shown as V2 in Figure 10, being the region across which the crack will propagate after the solder in region V1 has failed.

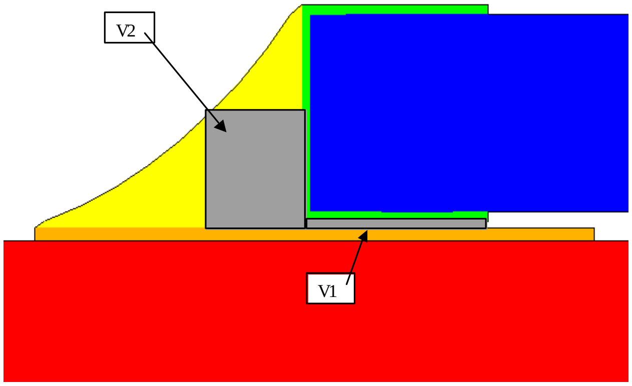

Fig 10: Schematic Showing Two Solder Regions

The total number of cycles for the crack to travel through the two regions (V1 and V2) was then calculated with the total lifetime being the sum of these results, shown in Table 2 for Cycle D, being a temperature cycle from –20ºC to +125ºC with a 7 minute period.

Table 2: Creep Strain Energy Based Results (Cycle D)

Cycles to failure, N_f	Region 1	Region 2	Total
Lu et al. [6]	201	5324	5525

The results clearly show that the solder fillet contributes most to the lifetime. Traditional analytical approaches to predicting the lifetime of a LCR or Leadless Ceramic Chip Carrier (LCCC) only consider the relative expansivity of the package and board, and the resulting shear strain in the solder layer under the package. No account is taken of the influence of the solder fillet, and so the analytical approach would be expected to drastically under predict the lifetime. However, using the results from an FE analysis allows the shear in the solder fillet to be considered, offering the possibility of obtaining much better results, providing the motivation for this study.

RESULTS OF THIS STUDY

Following the earlier methodology, the analysis was then carried out in two steps. First, the shear strain in the solder between the resistor and the board (region V1) was predicted. Second, the solder in this region was removed and the shear strain in fillet (region V1) was calculated. The geometry and material properties used for the analysis were identical to those used by Lu et al.[6], shown in Figure 5 and Table 1, with the exception that elastic material properties have been used to model the solder joint. Both the solder regions were found to be strained well beyond their yield strain, given by Getkin et al. [8] as 0.0002 at room temperature. To correct for the use of linear elastic properties beyond the yield point, the shear strains in the two regions were used to calculate an effective shear modulus for each, and hence an effective elastic modulus, to use to repeat the calculation. The process was repeated until the shear strain predicted was consistent with the effective elastic modulus used in the analysis.

For the solder between the resistor and the PCB, the shear strain was fairly uniform with a maximum value of 0.053. Under such conditions, where the calculated strain is much greater than the elastic limit, the elastic strain in the solder will be a very small proportion of the total strain. This allows the total shear strain to be considered to be equivalent to the plastic shear strain. This approach has been employed by Getkin et al. [8] to predict solder joint reliability from a linear elastic FE analysis.

In the second step, the solder in region V1 was not included to simulate the effect of the complete cracking of this region. The shear strain in region V2 is non-uniform, with a maximum value of 0.015 predicted in the corner of the fillet at the edge of the package. Figure 11 shows the shear strain through the solder fillet at the edge of the package along a diagonal from the bottom of the package to the surface of the fillet (i.e. diagonally across region V2), corresponding to the line of the fillet crack shown in Figure 9.

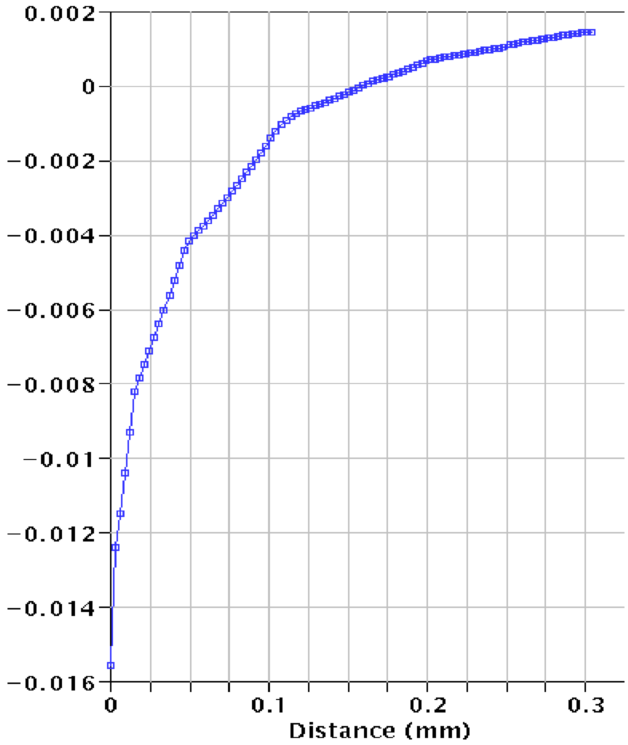

Fig. 11: Shear Strain Through Fillet Along Crack Path

For both these regions the maximum shear strain was used in the Coffin-Manson equation to predict the cycles to 50% population failure:

$$N_{50} = \frac{1}{2}\left(\frac{g_p}{2e_f}\right)^{(1/c)}$$

Where:
γ_p = plastic shear strain, approximated as total shear strain
ε_f = fatigue ductility coefficient
c = fatigue ductility exponent

Engelmaier [9] determined that for Sn60/Pb 40 solder that the fatigue ductility exponent can be represented by:

$$c = -0.442 - 0.0006T_s + 0.0174\ln\left(\frac{1+360}{t_D}\right)$$

Where:
T_s = mean cyclic solder joint temperature (ºC)
t_D = half cycle dwell time (minutes)

and the fatigue ductility coefficient, $\varepsilon_f = 0.325$.

The temperature cycle from Lu et al. [6] was –20ºC to +125ºC with a 7 minute period, which using the expression above gives: c = -0.390, giving the following results:

Table 3: Shear Strain Based Results (Cycle D)

	Region 1	Region 2	Total
Max. shear strain	0.053	0.015	-
Cycles to failure, N_{50}	309	7870	8179

DISCUSSION

Shear strain based results correctly shows that the solder fillet contributes most to the life of the part. This is considerably better than that which could be achieved by using an analytical model for the package, where only the solder under the resistor would be considered. However, use of the Coffin-Manson model for the fillet region requires some decision about the shear strain to use. In this study we have chosen to use the maximum value, since this corresponds to the failure site. However, as the crack propagates, the shear strain at the failure site will also change.

Comparing the results of Lu et al. [6] in Table 2 with those of the current study shown in Table 3 shows, the lifetime estimated by the shear strain based approach is around about 150% of that estimated using the creep strain energy approach. In both cases the cycles to failure in the region between the resistor and the PCB (V1) accounts only for about 4% of the total lifetime. This is the result of higher stress and strain in this part of the solder material.

The ability of the approach to predict the effect of design changes on the relative lifetime of the solder joint is of more interest than obtaining accurate the results for one geometry. For example a change in solder volume would change both the standoff height and the shape of the solder fillet. Lu et al. [6] noted that the stand-off height is important as it greatly affects the strain in the region between the resistor and the PCB, but since cracks spend much of their time to cross the fillet, the volume and shape of the solder fillet is perhaps even more important for the resistor's reliability. The shear strain based approach can account for the influence of the solder joint height on the lifetime of the part. However, unlike the creep strain energy based approach, the model does not take account of the number of cycles required for the crack to form, or does it have any concept of the distance across which the crack propagates.

Experiments are currently underway at the National Physics Laboratory, UK, that will provide experimental data on cycles to failure for the above resistor component using both Tin-Lead and Lead-free solders.

CONCLUSIONS

Both illustrative examples consider temperature cycles. The results of both studies have shown that reasonable results are obtained using the shear strain based Coffin-Manson model.

For the resistor case, the lifetime estimated by the shear strain based approach is around about 150% of that estimated using the creep strain energy approach.

For both the strain based and energy based approaches, the cycles to failure in the region between the resistor and the PCB accounts only for about 4% of the total lifetime. The stress and strain in the solder fillet is much lower than that between the resistor and the PCB and so accounts for the majority of the lifetime predicted.

The shear strain based approach is does not include any concept of the distance across which the crack propagates. This may limit its use for qualitative evaluation of design changes such as changes to solder volume.

FUTURE CHALLENGES

Using a more accurate representation of the thermal environment in the thermomechanical analysis may also lead to more accurate the stress data for use in reliability predictions, but this requires further research. Research in this subject has recently commenced through a 3-year European Community funded project, PROFIT (IST-1999-12529) which started in January 2000.

PROFIT aims to create methods and tools to enable rapid assessment of thermal parameters affecting yield, performance, reliability and safety in electronic equipment. However, analysis is seriously hampered by the lack of standard methods to predict temperature gradients in time and space, with sufficient accuracy. The industrial challenges and solutions offered by PROFIT are:

- Cost/weight reduction with better quality, via significant improvements in temperature prediction for virtual prototyping
- Physics-based prediction of reliability, via accurate prediction of temperature gradients in time and space
- Yield improvement of packages, via better-defined rejection criteria based on in-line quality testing
- Awareness of problems due to the absence of useful design specs, via dissemination of combined thermal expertise in Europe
- Standardisation of thermal characterisation, via European focal point to support international efforts.

Ultimately, the results of PROFIT will be suited for implementation in emerging virtual prototyping methods and physics-based reliability analysis software.

The PROFIT project is co-ordinated by Philips Research. The project consortium includes semiconductor manufacturers (Philips Semiconductors, Infineon Technologies, ST Microelectronics); system makers (Nokia, Philips); thermal analysis software vendors (Flomerics, MicRed); a statistics expert centre (Centre for Quantitative Methods); a university specializing in electrothermal analysis and transient measurements (Technical University of Budapest); and a major research institution contributing in the fabrication of test dies and tool integration (TIMA).

The work programme will focus on major improvements in thermal analysis throughout the design chain, from device via package and board to system. Novel test set-ups will be built in order to measure important parameters required for accurate numerical analysis, such as interface resistances, emissivities, local boundary conditions and local board thermal conductivities. Transient measurements at device and package level will be performed to assess data quality. Analysis of the data will be treated with novel, non-linear parameter estimation methods. Software will be improved, developed and integrated to facilitate the application of the project results in performance and reliability calculations. Various demonstrators showing the final deliverables are foreseen. The steady-state thermal characterisation of compact models will be extended to the transient domain. Yearly workshops will be organised to promote discussion amongst experts, and to facilitate early standardisation. In short, the innovative elements of the project are:

- Novel statistical approach for the optimisation of experiments, analysis of transient data and generation of dynamic compact models.
- Novel measurement techniques for the acquisition of input data.
- Novel electrothermal and thermomechanical board/system level software.
- New proposals for the standardisation of transient thermal characterisation.

During PROFIT, Flomerics will research into compact thermomechanical representations of thin and composite structures commonly found in electronics assemblies. The end user partners, Nokia and Philips, will compare the results of using data obtained from FLO/STRESS with existing in-house reliability prediction protocols.

ACKNOWLEDGEMENTS

FLO/STRESS has been developed in conjunction with the University of Greenwich, with partial funding provided by the UK Department of Trade and Industry under a TCS Programme (Grant #s 2341 and 2976).

REFERENCES

[1] John Parry, Chris Bailey, Chris Aldham, “Multiphysics Modelling For Electronics Design”, ITHERM2000, Las Vegas, p86-93, 2000

[2] M. Warner, J. Parry, C. Bailey, C. Marooney, H. Reeves, K. Pericleous, “FLO/STRESS: An Integrated Stress Solver for the CFD tool FLOTHERM”, Proceedings of IPACK 2001, July 8–13, 2001, Kauai, Hawaii, USA

[3] R. Darveaux “Solder Joint Fatigue Life Model”, Design and Reliability of Solders and Solder Interconnections, 1997, pp213-218, Pub TMS.

[4] “The National Technology Roadmap For Semiconductors”, Semiconductor Industry Association, 1997.

[5] John Parry, Harvey Rosten and Gary B. Kromann, “The Development of Component-level Thermal Compact Models of a C4/CBGA Interconnect Technology: The Motorola PowerPC 603 and PowerPC 604 RISC Microprocessors”, Transactions of IEEE CPMT, Vol. 21, No. 1, Mar. 1998, pp. 104-112

[6] H. Lu, C. Bailey, M. Dusek, C. Hunt and J. Nottay, “Modeling the Fatigue Life of Solder Joints for Surface Mount Resistors”, *International Symposium on Electronic Materials and Packaging*, Hong Kong, p136-143, Pub IEEE, ISBN 0-7803-6654-9, 2000

[7] PHYSICA, V2.10. http://physica.gre.ac.uk

[8] V. Getkin, A. Bar-Cohen and J Ames, “Coffin-Manson Fatigue Model of Underfilled Flip Chips”, IEEE Trans. Comp. Pack. & Man. Tech, Part A, Vol. 20, No. 3, pp. 317-325, 1997.

[9] W Englemaier, “Fatigue Life of Leadless Chip Carriers Using Manson-Coffin Equations”, IEEE Trans. Comp. Hybrids, & Man. Tech. Vol. CHMT-6, No. 3, pp. 232-237, Sept. 1983.